LA-6164-PR
Progress Report

C.3

Special Distribution
Issued: December 1975

Applied Nuclear Data Research and Development

July 1—September 30, 1975

Compiled by

C. I. Baxman
P. G. Young

los alamos
scientific laboratory
of the University of California
LOS ALAMOS, NEW MEXICO 87545

An Affirmative Action/Equal Opportunity Employer

UNITED STATES
ENERGY RESEARCH AND DEVELOPMENT ADMINISTRATION
CONTRACT W-7405-ENG. 36

The four most recent reports in this series, unclassified, are LA-5804-PR, LA-5944-PR, LA-6018-PR, and LA-6123-PR.

In the interest of prompt distribution, this report was not edited by the Technical Information staff.

This work was performed under the auspices of the Defense Nuclear Agency, The Nuclear Regulatory Commission, The National Aeronautics and Space Administration, and the U.S. Energy Research and Development Administration's Divisions of Military Application, Reactor Research and Development, Physical Research, and Controlled Thermonuclear Research.

CONTENTS

APPLIED NUCLEAR DATA RESEARCH AND DEVELOPMENT

QUARTERLY PROGRESS REPORT

July 1 — September 30, 1975

Compiled by

C. I. Baxman and P. G. Young

ABSTRACT

This progress report describes the activities of the Los Alamos Nuclear Data Group for the period July 1 through September 30, 1975. The topical content of this report is summarized in the Contents.

I. THEORY AND EVALUATION OF NUCLEAR CROSS SECTIONS

A. Analyses of Neutron-Induced Reactions on ^{15}N, ^{10}B, and ^{6}Li (G. M. Hale, E. D. Arthur, and P. G. Young)

The evaluation of cross sections for neutron-induced reactions on ^{15}N has been completed, and a tape was sent to the National Neutron Cross Section Center (NNCSC) at Brookhaven National Laboratory (BNL). As described in earlier progess reports, an R-matrix fit was made with the code EDA to total and differential cross sections[1,2] up to an energy of 5.4 MeV. Level assignments generally agreed with those of Zeitnitz et al.[1] except in the region of 4.0-4.15 MeV. From 4.5 to 5.4 MeV, tentative assignments were made. Angular distributions of neutrons resulting in excitation of the first eight levels of ^{15}N were calculated with the code COMNUC in the neutron energy region from 6 to 20 MeV. Also in this region, the secondary neutron, gamma-ray, and charged particle spectra were calculated with the statistical model code GNASH.

Work also began on the further R-matrix analysis of the $^{10}B(n,\alpha)$ reaction in the neutron energy range up to 1 MeV for incorporation into ENDF/B-V. This reaction is important because of its use as a neutron standard in this range. A previous R-matrix analysis incorporated mainly data from the $n + {}^{10}B \rightarrow n + {}^{10}B$, $n + {}^{10}B \rightarrow \alpha_0 + {}^{7}Li$, and $n + {}^{10}B \rightarrow \alpha_1 + {}^{7}Li$ reactions with a limited amount from $\alpha + {}^{7}Li$ reactions. The parameters obtained from this analysis did not produce a completely satisfactory fit, so a separate and more detailed analysis of the $\alpha + {}^{7}Li$ reactions was made.[3] The present effort centers around the incorporation of parameters determined from the $\alpha + {}^{7}Li$ analysis with the data from the neutron induced reactions on ^{10}B. Such an approach has an advantage in that several resonances which should affect the neutron channel in the regions of interest show up clearly in the $\alpha + {}^{7}Li$ channel. By including both types of data, it may be possible to overcome problems in the R-matrix analysis of the ^{11}B system arising from inconsistent data sets.

The analysis of $n + {}^{6}Li$ reactions described at the Washington Conference[3] was extended to include new total cross-section measurements from GEEL.[4] The results of this analysis were converted to ENDF/B format and are being submitted for the Version V ENDF/B standard cross-section file.

B. GNASH Code Development (E. D. Arthur, P. G. Young, and D. G. Foster, Jr.)

Recent work on the statistical model code GNASH has centered around the incorporation of options to improve computing speed and the implementation of a new pre-equilibrium model. The program now computes the compound nucleus formation cross section before the main program loop begins for cases where width fluctuation corrections[5] are not desired. For calcu-

lations involving medium or heavy nuclei, a factor of two reduction in computing time is achieved.

The pre-equilibrium model expression of Milazzo-Colli et al.[6] has been incorporated into the code and is now undergoing testing. The closed-form expression for pre-equilibrium ($d\sigma/d\varepsilon$) is absolutely normalized, and correctly detetermines the fraction of precompound processes as a function of incident particle energy. This model has been used to successfully analyze spectra and integrated cross sections from (n,α)(Ref. 6), and (n,p)(Ref. 7) reactions on medium and heavy nuclei.

Finally, other improvements to GNASH are in progress, which involve options for more automatic and preprogrammed functions so that fewer input parameters will have to be specified. For example, a data file containing mass tables and ground state spin-parity information for all nuclei is being constructed and will be accessed directly by GNASH.

C. Evaluation of ^{175}Lu(n,xn) Cross Sections (C. A. Philis [Bruyères-le-Châtel], P. G. Young, and E. D. Arthur)

As a continuation of (n,2n) and (n,3n) cross-section evaluation work begun at Bruyères-le-Châtel, we have evaluated experimental data on n + ^{175}Lu reactions between threshold and 20 MeV and performed statistical theory calculations with the model code GNASH. The available ^{175}Lu(n,2n) and (n,3n) experimental data were compiled and corrected to a modern (and consistent) set of standards for flux measurements, half-lives, and decay schemes.

For the GNASH calculations, the global optical model parameters of Wilmore and Hodgson[8] were used to generate neutron transmission coefficients, although some calculations were made with the tabulated transmission coefficients of Mani[9] for consistency checks. Gamma-ray transmission coefficients were calculated with the Brink-Axel giant dipole resonance form. The E1 gamma-ray strength was adjusted to give agreement with measured (n,γ) values in the range from 4 to 14 MeV. The shape and magnitude of the (n,2n) cross section near threshold was somewhat sensitive to the magnitude of the calculated capture cross section since competition between gamma-ray and neutron emission can be important in these regions.

With no adjustment of other parameters and without pre-equilibrium contributions, the solid curves shown in Fig. 1 were obtained from the GNASH code. The calculated (n,2n) results are in excellent agreement with the measurements of Frehaut[10] below 15 MeV. At higher energies, the calculated (n,2n) data are higher and the (n,3n) data lower than the Bayhurst[11] results. In addition, the calculated (n,2n) data are somewhat higher than preliminary measurements by Veeser.[15] The ENDF/B-IV evaluated data differ substantially from both the new measurements and the calculations above 15 MeV.

D. Discrepancies in (n,f) Measurements on ^{235}U, ^{238}U, and ^{239}Pu and Discrepancies in (n,γ) Measurements on ^{197}Au and ^{238}U (L. Stewart)

^{235}U is an accepted fission cross-section standard but recent measurements at other laboratories show fairly significant discrepancies with Los Alamos Scientific Laboratory (LASL) absolute experiments from 1 to 6 MeV. In addition, discrepancies are apparent in the energy calibration among the various experiments. These problems become severe in trying to determine both the shape and the magnitude of the important fissile and fertile cross sections.

Recently, intermediate structure has been observed in ^{235}U fission and ^{197}Au and ^{238}U capture cross sections up to 50-100 keV. ^{238}U capture cross sections measured at Karlsruhe and at Oak Ridge range from 10-20% higher than reported by BNL and Rensselaer Polytechnic Institute (RPI) below 100 keV.

All of the above are relevant to the problems of evaluating both the shape and magnitude of the ^{235}U fission and ^{197}Au capture standards for ENDF/B-V. The energy shift in data sets is apparent all the way to 20 MeV and is well outside the errors given by the experimentalists. While a shift in the energy scale will bring the cross sections into somewhat better agreement, it will not completely resolve the shape differences. A few of the recent measurements are well outside the values currently used in design studies. Therefore, further work is underway to try to understand these discrepancies in order to recommend changes for Version V of ENDF/B.

II. NUCLEAR CROSS-SECTION PROCESSING

A. MINX Code Development (R. E. MacFarlane and R. B. Kidman)

The MINX code is nearing completion, and procedures for release and reporting were established in consultation with C. R. Weisbin and J. E. White at Oak Ridge National Laboratory (ORNL). When ORNL has completed implementing the most recent updates to

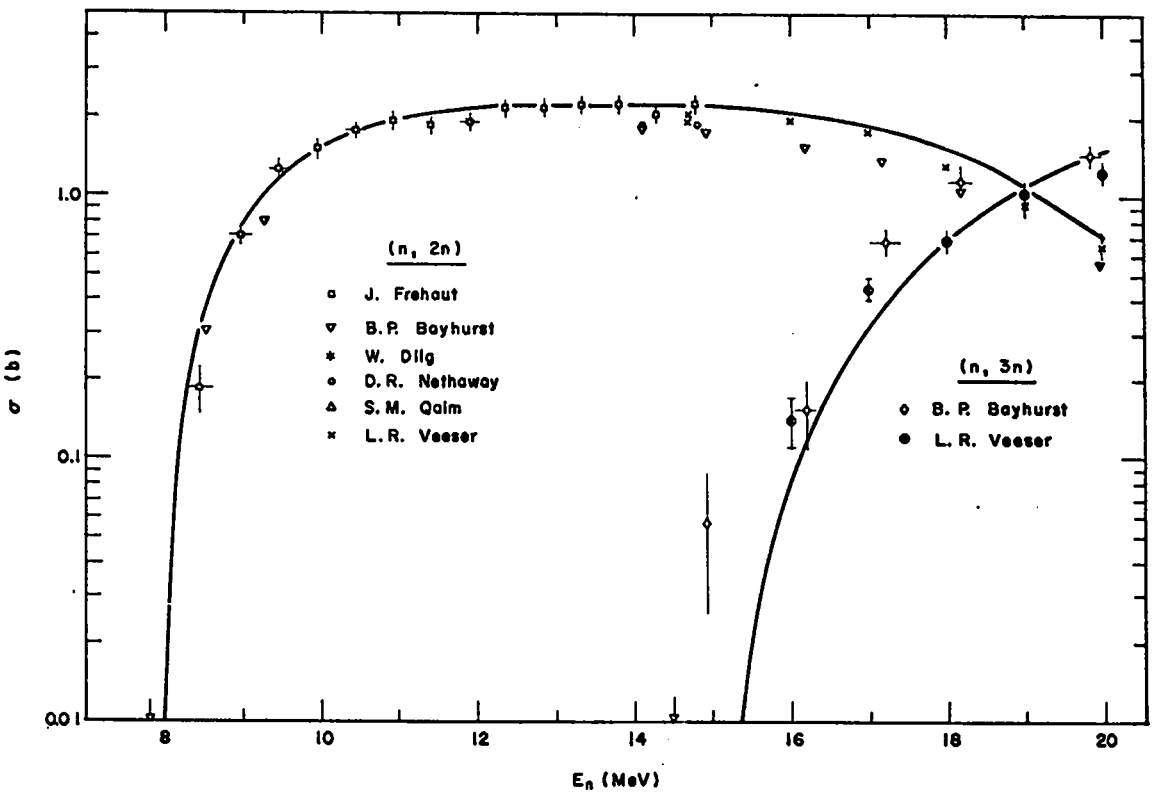

Fig. 1. ^{175}Lu(n,2n) and (n,3n) cross sections from threshold (arrows) to 20 MeV. The calculated curves are compared to the experimental results of Frehaut et al.,[10] Bayhurst et al.,[11] Dilg et al.,[12] Nethaway,[13] Qaim,[14] and Veeser.[15]

the MINX code, they will return to LASL the statements needed to make the code operate on their IBM machine. We will modify the code to include as many IBM features as possible and run the result through the TIDY code to obtain the final CDC-7600 version. The remaining modifications needed to make MINX run on the IBM machine will then be assembled into a modification set and returned to ORNL for final testing. Both versions of the code and the modification set will be provided to the Argonne Code Center. This procedure assures that the two versions of the code will be as identical as possible, with the differences clearly defined.

A draft of the report is being assembled at ORNL. It will be passed among the authors again starting in late November, and then published as a LASL report early in 1976.

The MINX code has been rearranged to isolate the Doppler broadening function and the production of CCCC[16] format output into their own overlays. This modification provides a more logical structure, allows the user's input to be collected into two new subroutines, and makes better use of storage and scratch tapes. An improved restart capability was added to the Doppler broadening module. This makes it possible to recover runs aborted by a time limit, or to add new temperatures to an existing data set at minimum cost. The MINX code was further improved by the addition to the RESEND[17] module of a new, faster method for reconstructing multi-level Breit-Wigner (MLBW) resonance cross sections. This method was developed by C. Lubitz (Knolls Atomic Power Laboratory [KAPL]) and coded by P. Rose (BNL).[18]

The MINX module, which computes group cross sections and f-factors, was edited and improved this quarter. A previously inoperable option to specify a list of reactions to be processed was corrected and activated. This required associated modifica-

tions in the handling of $\bar{\mu}$ and the transport cross section. The selective reaction capability was also added for the calculation of group-to-group transfer cross sections. Additional modifications to the Doppler broadening and group-averaging routines were found necessary for the processing of the incomplete evaluations of the fission product cross sections (ENDF/B-IV tapes 414-419).

Other miscellaneous improvements and corrections made this quarter include: more reduction in printed output, a correction to the calculation of potential and interference scattering in the unresolved range for multi-isotope materials, a correction to the calculation of the center-of-mass (CM) to laboratory transformation matrix for discrete inelastic scattering, the calculation of CM Legendre coefficients at or below the reaction threshold, and a modification to the energy grid produced during linearization. This last change was in two parts. A minimum lethargy step was defined to prevent the use of too many points at thresholds specified by log-log interpolation, and a maximum lethargy step was specified to assure that long linear-linear or constant segments will have enough points for accurate Doppler broadening by the point kernel method.[19]

B. NJOY Code Development (R. E. MacFarlane, R. M. Boicourt, and R. J. Barrett)

The development of the NJOY nuclear cross-section processing code continued this quarter with the initiation of several new modules and significant additions to existing ones.

A complete plotting capability has been added to the DTFR module. Each edit cross section requested plus the three standard DTF (Ref. 20) edits (σ_a, $\nu\sigma_f$, and σ_t) are plotted vs energy with the corresponding point cross section (if any) overlayed. If an edit contains more than one point cross section, all are overlayed together. In addition, the P_0 tables for neutron scattering and photon production are presented as isometric plots.

The GROUPR module which generates all $n \rightarrow n$ and $n \rightarrow \gamma$ cross sections has been extended to allow for histogram data and other discontinuous functions. This addition will enable NJOY to average group-wise data in ENDF/B format in addition to the limited amount of histogram data in ENDF/B-IV. The processing of delayed neutron spectra and yields was reactivated.

For comparison and testing purposes, the RESEND (Ref. 17) and SIGMA1 (Ref. 19) codes have been converted to the NJOY input/output system and installed as modules. RESEND has also been modified to include the new MLBW resonance reconstruction method,[18] psi-chi Doppler-broadened reconstruction of SLBW resonances, and the new unresolved resonance quadrature scheme.[21] An abbreviated version of NJOY containing these two modules is to be implemented at BNL as a test of exportability and to demonstrate the usefulness of blocked binary ENDF/B tapes.

For most applications using NJOY, the functions of resonance reconstruction and Doppler broadening will be performed by the RECONR and BROADR modules. RECONR uses the resonance reconstruction methods of RESEND, but produces cross sections on a linearized and unionized grid. This representation is useful for continuous energy Monte Carlo codes, allows for accurate Doppler broadening by the point kernel method, and improves the accuracy of self-shielded group-averaged cross sections. The coding also provides for psi-chi broadened resonance reconstruction. The BROADR module uses the method of SIGMA1 (Ref. 19), but takes advantage of the union grid to broaden and thin several reactions simultaneously and does not broaden or thin threshold reactions at all. It includes a flexible restart capability and a *bootstrap* option so that each broadening step can begin from the results at the previous temperature, if desired. These two routines are now being tested and debugged.

The output of these two modules will be used by GROUPR to generate group-averaged cross sections. It can also be used by the new MCNR module to generate cross sections for the LASL continuous-energy Monte Carlo code MCN (Ref. 22). The data are already on the unionized and linearized grid required by MCN, but the photon production cross sections must be summed into a single cross section on the union grid. The neutron angle and secondary energy distribution functions are converted into equal probability bins using a program TOPFIL converted to NJOY input/output from ETOPL (Ref. 23). Photon production will be represented by a set of equally probable photon mean-energies using a new routine. The MCNR data are written to an output tape in ENDF format (the format for photon distributions has yet to be defined).

Group cross sections and transfer matrices can be used by many reactor design codes if they are ex-

pressed in the CCCC-III interface format.[16] NJOY results from GROUPR will be formatted using the new CCCC module. This program will have several improvements over the MINX output module. It will be able to generate multi-isotope files directly from the GROUPR output tape; they will include the ISOTXS isotope cross-section file, the BRKOXS self-shielding factor file, the DLAYXS delayed neutron file, and a new photon production and interaction file designed to make self-shielded photon production capabilities available to the space-energy collapse code SPHINX. In the new module, scattering matrices can be written in two different forms which can be selected by the user:

1. The scattering matrix is organized in up to four blocks, one for each reaction type (inelastic, elastic, n2n, and total). Each block may be divided into sub-blocks by sink group, if necessary, with each sub-block containing all Legendre orders and source groups for that sink group. This is the only option available in MINX.
2. Here a block is defined for each scattering order (ℓ-order) within each reaction type. Each block contains all combinations of sink and source groups. Such a block can be divided into sub-blocks by sink group, if necessary.

The ISOTXS capability has been coded and is being tested.

We have begun to work on the problem of including a photon interaction processing capability in NJOY. It will include the functions of GAMLEG (Ref. 24) and add the ability to process the photon scattering form factors[25] now available in ENDF/B-IV. R. Barrett has been appointed to an interlaboratory task force under the jurisdiction of the Cross Section Evaluation Working Group (CSEWG) Shielding Subcommittee. This group has been charged with investigating several problems associated with the processing and utilization of photon interaction data.

C. Code Comparison Testing (R. E. MacFarlane and R. E. Seamon [TD-6])

The code comparison effort this quarter had concentrated on the comparison and validation of the photon production capabilities of NJOY and LAPHANO (Ref. 26). This effort was carried on through the CSEWG Shielding Subcommittee and included participation by ORNL and General Atomic (GA). Although the test problems originally specified were not easily implemented with NJOY, it was discovered that NJOY did not handle the "LP flag" correctly, and that LAPHANO did not handle transition probability arrays correctly.

The LP flag is used to conserve energy in capture reactions by including the CM kinetic energy in the energy of the emitted photon. This effect has been coded into GROUPR.

The problem with the transition probability arrays (File 12, LO = 2) apparently goes back to the LAPH code[27] and the earlier ENDF/B format it was designed to process. In this format, photon yields from known levels were separated from yields from higher lying levels by stating that level decay schemes were not to be used for energies larger than the threshold for the highest level given. This condition has survived into LAPHANO and results in no contributions being counted for the highest level (e.g., MT 68 for Na-23, MAT 1156).

The manual describing the current format[28] contains no mention of such a cut-off. In fact, other statements say that the contributions from all reactions are to be added and that there shall be no redundancies in the file. Therefore, the yields from the highest known level must be counted, as is done in the NJOY code.

Detailed comparisons have been carried out between NJOY, LAPHANO, and hand calculations using identical 1/E weight functions and pointwise data tapes generated by MINX for ^{6}Li, ^{23}Na, and F.

D. Processed Cross-Section Production (R. B. Kidman)

A 50-group, 92-material library (LIB IV) has been generated with MINX from ENDF/B-IV. The materials and some salient characteristics of LIB IV are shown in Table I. The LIB IV group structure is shown in Table II. The purpose of this library is to provide the nuclear community with the first extensive tested set of MINX-processed cross sections. LIB IV represents a complete processing of ENDF/B-IV (except for the dosimetry tape) plus ^{63}Cu and ^{65}Cu from ENDF/B-III. LIB IV is distinct from the preliminary 22-isotope libraries generated in the two previous quarters in that it was generated with tighter convergence criteria, and it contains all MINX corrections, including the corrections mentioned in this quarterly report.

TABLE I

50-GP MATERIALS GENERATED WITH MINX FROM ENDF/B-IV[a]

	MATERIAL	ENDF/B MAT NO.	PHOTOSTORE NAME (+ VERSION) ISOTXS + BRKOXS	PENDF	MINX TIMING (SEC)	SIGO'S (BARNS)
1	H-1	1269	H1 (1)	H1P (1)	133	1000,100,10,1,.1,.01
2	H-2	1120	H2 (1)	H2P (1)	95	1000,100,10,1,.1,.01
3	H-3	1169	H-3 (1)	H3P (1)	165	1000,100,10,1,.1,.01
4	HE-3	1146	HE3 (1)	HE3P (1)	102	10000,1000,100,10,1,.1
5	HE-4	1270	HE4 (1)	HE4P (1)	118	10000,1000,100,10,1,.1
6	LI-6	1271	LI6 (1)	LI6P (1)	157	1000,100,10,1,.1,.01
7	LI-7	1272	LI7 (1)	LI7P (1)	159	1000,100,10,1,.1,.01
8	BE-9	1289	BE9 (4)	BE9P (3)	516	1000,100,10,1,.1,.01
9	B-10	1273	B10 (3)	B10P (3)	428	1000,100,10,1
10	B-11	1160	B11 (6)	B11P (5)	182	100000,10000,1000,100,10,1
11	C-12	1274	C12 (4)	C12P (4)	156	1000,100,10,1,.1
12	N-14	1275	N14 (1)	N14P (1)	593	1000,100,10,1,.1,.01
13	O-16	1276	O16 (3)	O16P (1)	590	1000,100,10,1,.1
14	F	1277	F (1)	FP (1)	442	10000,1000,100,10,1,.1
15	NA-23	1156	NA23 (3)	NA23P (2)	667	1000,100,10,1,.1
16	MG	1280	MG (1)	MGP (1)	584	10000,1000,100,10,1,.1
17	AL-27	1193	AL27 (2)	AL27P (2)	631	100000,10000,1000,100,10,1
18	SI	1194	SI (1)	SIP (1)	603	10000,1000,100,10,1,.1
19	CL	1149	CL (1)	CLP (1)	438	10000,1000,100,10,1,.1
20	K	1150	K (1)	KP (1)	387	10000,1000,100,10,1,.1
21	CA	1195	CA (1)	CAP (1)	599	10000,1000,100,10,1,.1
22	TI	1286	TI (3)	TIP (4)	218	100000,10000,1000,100,10,1
23	V	1196	V (1)	VP (1)	344	100000,10000,1000,100,10,1
24	CR	1191	CR (3)	CRP (3)	1721	1000,100,10,1,.1
25	MN-55	1197	MN55 (2)	MN55P (2)	635	100000,10000,1000,100,10,1
26	FE	1192	FE (5)	FEP (3)	1172	1000,100,10,1,.1
27	CO-59	1199	CO59 (2)	CO59P (2)	909	10000,1000,100,10,1,.1
28	NI	1190	NI (3)	NIP (3)	1268	1000,100,10,1,.1
29	CU	1295	CU (2)	CUP (2)	707	100000,10000,1000,100,10,1
30	[b]CU-63	1085	CU63 (1)	CU63P (1)	445	100000,10000,1000,100,10,1
31	[b]CU-65	1086	CU65 (1)	CU65P (1)	363	100000,10000,1000,100,10,1
32	KR-78	1181	KR78 (1)	KR78P (1)	148	10000,1000,100,10,1,.1
33	KR-80	1182	KR80 (1)	KR80P (1)	171	10000,1000,100,10,1,.1
34	KR-82	1183	KR82 (1)	KR82P (1)	180	10000,1000,100,10,1,.1
35	KR-83	1184	KR83 (1)	KR83P (1)	190	10000,1000,100,10,1,.1
36	KR-84	1185	KR84 (1)	KR84P (1)	218	10000,1000,100,10,1,.1
37	KR-86	1186	KR86 (1)	KR86P (1)	157	10000,1000,100,10,1,.1
38	ZIRC-2	1284	ZIRC2 (1)	ZIRC2P (1)	920	10000,1000,100,10,1,.1
39	NB-93	1189	NB93 (1)	NB93P (1)	3000	100000,10000,1000,100,10,1
40	MO	1287	MO (5)	MOP (4)	514	100000,10000,1000,100,10,1
41	TC-99	1137	TC99 (1)	TC99P (1)	333	100000,10000,1000,100,10,1
42	RH-103	1125	RH103 (1)	RH103P (1)	2412	100000,10000,1000,100,10,1
43	AG-107	1138	AG107 (1)	AG107P (1)	761	100000,10000,1000,100,10,1
44	AG-109	1139	AG109 (1)	AG109P (1)	779	100000,10000,1000,100,10,1
45	CD	1281	CD (1)	CDP (1)	841	10000,1000,100,10,1,.1
46	CD-113	1282	CD113 (1)	CD113P (1)	612	10000,1000,100,10,1,.1
47	XE-124	1170	XE124 (1)	XE124P (1)	164	10000,1000,100,10,1,.1
48	XE-126	1171	XE126 (1)	XE126P (1)	142	10000,1000,100,10,1,.1
49	XE-127	1172	XE127 (1)	XE127P (1)	297	10000,1000,100,10,1,.1
50	XE-128	1173	XE128 (1)	XE128P (1)	1155	10000,1000,100,1,.1
51	XE-130	1174	XE130 (1)	XE130P (1)	280	10000,1000,100,1,.1
52	XE-131	1175	XE131 (1)	XE131P (1)	741	10000,1000,100,1,.1
53	XE-132	1176	XE132 (1)	XE132P (1)	206	10000,1000,100,1,.1
54	XE-134	1177	XE134 (1)	XE134P (1)	135	10000,1000,100,1,.1
55	XE-135	1294	XE135 (1)	XE135P (1)	138	100000,10000,1000,100,10,1
56	XE-136	1178	XE136 (1)	XE136P (1)	119	100000,10000,1000,100,10,1
57	CS-133	1141	CS133 (1)	CS133P (1)	1459	100000,10000,1000,100,10,1
58	SM-149	1027	SM149 (1)	SM149P (1)	528	100000,10000,1000,100,10,1
59	EU-151	1290	EU151 (3)	EU151P (2)	884	100000,10000,1000,100,10,1
60	EU-152	1292	EU152 (3)	EU152P (2)	704	100000,10000,1000,100,10,1
61	EU-153	1291	EU153 (3)	EU153P (2)	788	100000,10000,1000,100,10,1
62	EU-154	1293	EU154 (3)	EU154P (3)	579	100000,10000,1000,100,10,1
63	GD	1030	GD (1)	GDP (1)	378	100000,10000,1000,100,10,1

TABLE I (Cont.)

50-GP MATERIALS GENERATED WITH MINX FROM ENDF/B-IV[a]

MATERIAL	ENDF/B MAT NO.	PHOTOSTORE NAME (+ VERSION) ISOTXS + BRKOXS	PENDF	MINX TIMING (SEC)	SIGO'S (BARNS)
64 DY-164	1031	DY164 (1)	DY164P (1)	210	100000,10000,1000,100,10,1
65 LU-175	1032	LU175 (1)	LU175P (1)	351	100000,10000,1000,100,10,1
66 LU-176	1033	LU176 (1)	LU176P (1)	380	100000,10000,1000,100,10,1
67 TA-181	1285	TA181 (4)	TA181P (4)	1081	10000,1000,100,1,.1
68 TA-182	1127	TA182 (1)	TA182P (1)	289	10000,1000,100,1,.1
69 W-182	1128	W182 (2)	W182P (2)	1889	100000,10000,1000,100,10,1
70 W-183	1129	W183 (2)	W183P (2)	1219	100000,10000,1000,100,10,1
71 W-184	1130	W184 (2)	W184P (2)	1213	100000,10000,1000,100,10,1
72 W-186	1131	W186 (2)	W186P (2)	1339	100000,10000,1000,100,10,1
73 RE-185	1083	RE185 (2)	RE185P (2)	468	100000,10000,1000,100,10,1
74 RE-187	1084	RE187 (2)	RE187P (2)	415	100000,10000,1000,100,10,1
75 AU-197	1283	AU197 (2)	AU197P (2)	1689	100000,10000,1000,100,10,1
76 PB	1288	PB (2)	PBP (2)	749	10000,1000,100,1,.1
77 TH-232	1296	TH232 (5)	TH232P (2)	3826	100000,10000,1000,100,10,1
78 PA-233	1297	PA233 (1)	PA233P (1)	450	100000,10000,1000,100,10,1
79 U-233	1260	U233 (5)	U233P (5)	503	10000,1000,100,1,.1
80 U-234	1043	U234 (2)	U234P (2)	663	100000,10000,1000,100,10,1
81 U-235	1261	U235 (2)	U235P (2)	1936	10000,1000,100,1,.1
82 U-236	1163	U236 (2)	U236P (2)	767	100000,10000,1000,100,10,1
83 U-238	1262	U238 (8)	U238P (13)	6040	10000,1000,100,1,.1
84 NP-237	1263	NP237 (2)	NP237P (2)	2290	100000,10000,1000,100,10,1
85 PU-238	1050	PU238 (2)	PU238P (2)	544	100000,10000,1000,100,10,1
86 PU-239	1264	PU239 (5)	PU239P (2)	2637	10000,1000,100,10,1
87 PU-240	1265	PU240 (2)	PU240P (2)	5544	100000,10000,1000,100,10,1
88 PU-241	1266	PU241 (4)	PU241P (4)	543	100000,10000,1000,100,10,1
89 PU-242	1161	PU242 (4)	PU242P (4)	651	100000,10000,1000,100,10,1
9 AM-241	1056	AM241 (1)	AM241P (1)	337	100000,10000,1000,100,10,1
91 AM-243	1057	AM243 (1)	AM243P (1)	231	100000,10000,1000,100,10,1
92 CM-244	1162	CM244 (1)	CM244P (1)	1028	100000,10000,1000,100,10,1
			TOTAL	74748	

[a]All materials in this table were run for the three temperatures 300, 900, and 2100°K. All materials except U-238, RH-103, and CS-133 were run with the following MINX tolerances: Reconstruction = 0.005; Linearization = 0.002; Doppler thinning = 0.002; Integration = 0.001. The three exceptions used a Reconstruction tolerance of 0.01. Finally, the smooth weighting function used in MINX was a thermal spectrum (with a Maxwellian temperature of 0.025 eV) up to 0.1 eV, a 1/E spectrum up to 0.8208 MeV, and a fission spectrum (with a nuclear temperature of 1.4 MeV) above 0.8208 MeV.

[b]These materials came from ENDF/B-III.

Current plans are to make LIB IV a referenceable library and release it to BNL for general distribution. This will be done only after LIB IV has been thoroughly compared with other processing code results, and after it has been used to calculate the CSEWG benchmarks. This testing is in progress.

All of the MINX run outputs from the generation of LIB IV are available on microfiche.

E. Phase II Testing of ENDF/B-IV Data (R. B. Kidman, R. J. Barrett, R. J. LaBauve, and W. B. Wilson)

The various laboratories participating in the Phase II testing of ENDF/B-IV data (Argonne National Laboratory, Brookhaven National Laboratory, General Atomic, General Electric, Hanford Engineering Development Laboratory, Los Alamos Scientific Laboratory, Oak Ridge National Laboratory, and Westinghouse) are documenting their results as a report to CSEWG. We have completed LASL's assignments and have sent our written portion on to Argonne National Laboratory (ANL) who will combine the various laboratory contributions into the final document.

TABLE II

LIB-IV GROUP STRUCTURE

GROUP	ENERGY RANGE		LETHARGY
01	1.5000E+07	1.0000E+07	0.692
02	1.0000E+07	6.0653E+06	0.5
03	6.0653E+06	3.6788E+06	0.5
04	3.6788E+06	2.2313E+06	0.5
05	2.2313E+06	1.3534E+06	0.5
06	1.3534E+06	8.2085E+05	0.5
07	8.2085E+05	4.9787E+05	0.5
08	4.9787E+05	3.8774E+05	0.25
09	3.8774E+05	3.0197E+05	0.25
10	3.0197E+05	2.3518E+05	0.25
11	2.3518E+05	1.8316E+05	0.25
12	1.8316E+05	1.4264E+05	0.25
13	1.4264E+05	1.1109E+05	0.25
14	1.1109E+05	8.6517E+04	0.25
15	8.6517E+04	6.7379E+04	0.25
16	6.7379E+04	5.2475E+04	0.25
17	5.2475E+04	4.0868E+04	0.25
18	4.0868E+04	3.1828E+04	0.25
19	3.1828E+04	2.4788E+04	0.25
20	2.4788E+04	1.9305E+04	0.25
21	1.9305E+04	1.5034E+04	0.25
22	1.5034E+04	1.1709E+04	0.25
23	1.1709E+04	9.1188E+03	0.25
24	9.1188E+03	7.1017E+03	0.25
25	7.1017E+03	5.5308E+03	0.25
26	5.5308E+03	4.3074E+03	0.25
27	4.3074E+03	3.3546E+03	0.25
28	3.3546E+03	2.6126E+03	0.25
29	2.6126E+03	2.0347E+03	0.25
30	2.0347E+03	1.5846E+03	0.25
31	1.5846E+03	1.2341E+03	0.25
32	1.2341E+03	9.6112E+02	0.25
33	9.6112E+02	7.4852E+02	0.25
34	7.4852E+02	5.8295E+02	0.25
35	5.8295E+02	4.5400E+02	0.25
36	4.5400E+02	3.5358E+02	0.25
37	3.5358E+02	2.7536E+02	0.25
38	2.7536E+02	1.6702E+02	0.5
39	1.6702E+02	1.0130E+02	0.5
40	1.0130E+02	6.1442E+01	0.5
41	6.1442E+01	3.7267E+01	0.5
42	3.7267E+01	2.2603E+01	0.5
43	2.2603E+01	1.3710E+01	0.5
44	1.3710E+01	8.3153E+00	0.5
45	8.3153E+00	5.0435E+00	0.5
46	5.0435E+00	3.0590E+00	0.5
47	3.0590E+00	1.8554E+00	0.5
48	1.8554E+00	1.1254E+00	0.5
49	1.1254E+00	6.8256E+01	0.5
50	6.8256E+01	1.0000E+05	11.31

III. DOUBLE-HETEROGENEITY TREATMENTS FOR GENERATING HTGR SPACE-SHIELDED CROSS SECTIONS (M. G. Stamatelatos and R. J. LaBauve)

A. Cross-Section Generation

The previously reported[29] route for generating cross sections for HTGR safety research at LASL used modified versions of the MC^2-I (Ref. 30) and Glen[31] codes, together with TOR[32] and HEXSCAT[33] for graphite. Cross sections generated with these codes did not take into account the space shielding effects of the doubly-heterogeneous structure of the fuel-moderator system in an HTGR. In order to account for these self-shielding effects, as well as to better account for energy self-shielding effects due to large concentrations of heavy absorbers in the fuel, an alternate route has been adopted. This route used MINX[34] together with a modified version of the 1DX[35] code adapted to handle the Bondarenko energy self-shielding formalism provided by MINX in the above-thermal region. The thermal region cross sections are still being generated with a modified version of the GLEN code.

The new procedure is as follows:

1. Use MINX to generate pointwise (PENDF) cross sections in the ENDF format for the entire energy region.

2. Run the PETOPES[36] program to particle (grain)-self-shield the PENDF cross sections for important heavy absorbers (e.g., ^{232}Th, ^{235}U) in the entire region (14-0 MeV).

3. Use MINX to collapse the PENDF cross sections to two fine-group energy structures, one in the above-thermal region (14 MeV-0.414 eV) and the other in the thermal region (2.38-0 eV). These cross sections are already grain shielded.

4. In the above-thermal region, run 1DX to collapse the fine-group cross sections to a broad-group structure. Gross heterogeneity (pin/moderator) corrections on the absorber cross sections are applied at this stage.

5. In the thermal region, run GLEN to calculate a thermal flux and to collapse the MINX thermal fine-group grain-shielded cross section to a broad-group structure.

6. DTF - format the broad-group cross sections.

For different temperatures, only steps 3 through 6 need be repeated.

B. Grain-Shielding Treatment

The grain-shielding procedure adopted is that used by Wälti[37] which is apparently being used in the General Atomic (GA) code MICROX.[38] This procedure was claimed by Wälti to agree very well with the detailed Nordheim integral transport treatment used in GAROL[39] and in the GGC-5 code[40] which contains GAROL.

In the Wälti procedure, the grain-shielded absorber microscopic cross section is given by

$$\sigma_i^{eff}(E) = \sigma_i(E) \frac{\Gamma(E)}{1-r^3[1-\Gamma(E)]} \quad , \qquad (1)$$

where $\sigma_i(E)$ = unshielded cross section for the i-th heavy nuclide;

r = ratio of fuel to moderator radii in a two-concentric-sphere model (inner = fuel; outer = moderator) representing a uniform grain distribution in the fuel rod; and

$\Gamma(E)$ = self-shielding factor, i.e., the ratio of average neutron fluxes in the grain and in the moderator, $\bar{\phi}_0/\bar{\phi}_1$, where subscripts 0 and 1 refer to the grain and the surrounding moderator regions, respectively.

If isotropic angular fluxes are assumed for regions 0 and 1, the neutron balance equations for the two regions yield

$$\Gamma(E) \equiv \frac{\bar{\phi}_0}{\bar{\phi}_1} = \frac{1+\rho\ Q[1+W\bar{\ell}_1(\Sigma_{a,1}+\Sigma_{out,1})]}{1+\rho\ Q+W\bar{\ell}_0(\Sigma_{a,0}+\Sigma_{out,0})} \qquad (2)$$

where $\rho = \dfrac{\bar{\ell}_0}{\bar{\ell}_1} = \dfrac{V_0}{V_1}$ = volume ratio of regions 0 and 1,

Q = ratio of spacially averaged source densities in regions 0 and 1,

$$W = 1 + \bar{H}_0(\Sigma_{t,0}) + \bar{H}_1(\Sigma_{t,1}) \quad , \qquad (3)$$

$\bar{\ell}_0$ and $\bar{\ell}_1$ are the mean chordlengths in regions 0 and 1, respectively:

$$\bar{\ell}_j = \frac{4V_j}{S_j} \quad , \quad j = 0,1 \quad , \qquad (4)$$

$\bar{H}_j$ = first-collision "augment" for region j:

$$\bar{H}_j(\Sigma_{t,j}) = \frac{1-\bar{P}_j}{\bar{\ell}_j\bar{P}_j\Sigma_{t,j}} \quad , \quad j = 0,1 \quad , \qquad (5)$$

$\Sigma_{a,j}$, $\Sigma_{out,j}$, and $\Sigma_{t,j}$ are the macroscopic absorption, outscatter, and total cross sections, repectively, for region j (0 or 1).

$\bar{H}_1(\Sigma_t)$ is approximated by $\bar{H}_1(0)$:

$$\bar{H}_1(0) = \left(\frac{\gamma}{r}\right)^2 \left\{\left(1-r^2\right)^2 \left(1+\frac{1}{4}\ \ell n\ \frac{1+r}{1-r}\right) - \frac{r}{2}\left(1-r\right)^2 + \left(\frac{2}{3r}\right)^2 \left[\left(1-r^2\right)^3 - 3\left(1-r^3\right)^2 + 2\left(1-r^3\right)\left(1-r^2\right)^{3/2}\right]\right\} \quad , \qquad (6)$$

where

$$\gamma = \frac{3r^2}{4\left(1-r^3\right)} \quad . \qquad (7)$$

$\bar{P}_0$ is given by the expression[41]

$$\bar{P}_0(\Sigma_{t,o}) = \frac{3}{8X^3}\left[2X^2-1 + (1+2X)\exp(-2X)\right], \qquad (8)$$

where

$$X = \frac{3}{4}\bar{\ell}_0\Sigma_{t,0} \quad . \qquad (9)$$

Q is given by

$$Q = \frac{\xi_{0,pot}\Sigma_{s,0}^{pot}}{\xi_{1,pot}\Sigma_{s,1}^{pot}} \quad , \qquad (10)$$

and the self-scattering cross section is approximated by

$$\Sigma_{ss,j}(E) \approx \frac{1-\xi_j(E)}{\xi_1^{pot}}\Sigma_{s,j}(E) \quad , \qquad (11)$$

where the average logarithmic energy decrement $\xi_j(E)$ is given by

$$\xi_j(E) = \frac{\sum_i \xi_j^i \Sigma_{s,j}^i(E)}{\Sigma_{s,j}(E)} \quad , \quad j = 0,1 \quad , \qquad (12)$$

i being the nuclide index.

Derivation of these equations and justifications of the approximations used can be found in Ref. 37.

A computer program PETOPES was written to apply the above formalism to pointwise cross sections generated by MINX. The PETOPES code transfers MINX-generated PENDF cross sections into grain-shielded PENDF cross sections which can be processed by MINX. Results of the PETOPES program agree very well with those published by Wälti[37] for the ThC_2 grain structure of the Fort St. Vrain (FSV) HTGR.

C. Fuel Pin Heterogeneity Treatment

The escape probability from a regular array of fuel (absorber) lumps, each assumed homogeneous in composition, is given by the usual expression

$$P^*_{esc} = P_{esc} \frac{1-C}{1-C(1-\Sigma_F \bar{\ell}_F P_{esc})} , \qquad (13)$$

where P_{esc} = escape probability from one lump,
C = Dancoff factor, and
$\bar{\ell}_F$ = fuel-rod mean chordlength

Equations for P_{esc} for various lump geometries have been derived by many investigators (e.g., see Refs. 41, 42, and 43). Wigner[44] has proposed a *rational* approximation for P_{esc} which gives the correct value for very large or very small lumps. For better approximations between the two extreme limits, various Wigner-like approximations have been proposed. One popular version is due to Levine[45]

$$P_{esc} \simeq \frac{1}{1+\frac{\Sigma_F \bar{\ell}_F}{A}} , \qquad (14)$$

where A = Levine factor (pin-geometry dependent).

For cylindrical pins, Otter[46] has found that the energy-independent value 1.35 for A works quite well for a large range of fuel-pin radii. If Eq. (14) is substituted into Eq. (13), it can be shown that P^*_{esc} can be written

$$P^*_{esc} = \frac{1}{1+\frac{\Sigma_F}{\Sigma_e}} , \qquad (15)$$

where the effective cross section Σ_e is given by

$$\Sigma_e = \frac{(1-C)A}{\bar{\ell}_F[1+C(A-1)]} . \qquad (16)$$

The advantage of the rational form of Eq. (15) is the equivalence between the heterogeneous system and a homogenized system for which the moderator cross section is equal to the moderator cross section in the fuel pin of the heterogeneous system, plus the effective cross section Σ_e.[47,48] This implies that pin heterogeneity corrections to cross sections can be made by simply adding Σ_e to the moderator cross section in the fuel and treating the system as homogeneous.

This formalism has already been included in a modified version of the 1DX code.

D. Alternate Simplified Double-Heterogeneity Treatment

Preliminary calculations have shown successful results with a considerably simplified method for treating the double heterogeneity in HTGR fuel pins without need of first grain-shielding cross sections at the PENDF level as discussed above. This method, an extension of the pin heterogeneity correction method, is designed to be used as a rapid independent check of the more elaborate method discussed above. Full details will be reported in the near future.

IV. NUCLEAR DATA FOR CTR APPLICATIONS -- SIMULATION OF 14-MeV NEUTRON DAMAGE WITH HIGH-ENERGY PROTONS (D. W. Muir and J. M. Bunch [CMB-5])

High-energy protons are a potentially useful tool for simulating the radiation damage produced by 14-MeV neutrons in fusion reactor (CTR) materials. In order to shed some light on the similarities and differences between the damage produced by these two types of radiation, we have performed a theoretical analysis of a radiation damage experiment performed on the CTR candidate-insulator, Al_2O_3.

The experiment made use of the prominent optical absorption band at 206 nm as an index of lattice damage, on the assumption that peak absorption is proportional to the concentration of lattice vacancies. The induced absorption was measured for incident proton energies ranging from 5 to 15 MeV and for 14-MeV neutrons.

As the first step in our analysis, we reviewed the available proton interaction data for ^{27}Al and ^{16}O for proton energies up to 15 MeV. (This step was not necessary for 14-MeV neutrons, since complete evaluations of neutron cross sections for these materials are available in ENDF/B.[49,50])

Because of factors related to charge and mass of the projectile, the direct proton beam causes much less permanent lattice damage than target nuclei recoiling from elastic and nonelastic reactions in the samples. Thus, one needs to know the energy dependence of all major reaction cross sections, as well as the angular distribution of the reaction products, since the latter determines the energy spectrum of the recoiling heavy ions. The results of our review of the proton interaction cross sections are described in some detail in Ref. 51, which also contains a description of the remaining theoretical analysis of the relative damage effectiveness of 14-MeV neutrons and 0-15 MeV protons.

A summary of the results of our analysis is given in Table III. The energy of the incident protons is given in the first column (ionization energy losses in the sample were 2-3 MeV). In the second column is given the ratio of the measured damage effectiveness of protons of each energy to that of 14-MeV neutrons. In the third column, the theoretical values of these ratios are given. The relatively good agreement between the measured and calculated ratios suggests that the models commonly used to describe fast-neutron radiation damage[52] are adequate to describe high-energy proton damage as well.

TABLE III

PROTON DAMAGE EFFECTIVENESS RELATIVE TO 14-MeV NEUTRONS

Proton Energy	Experimental Ratio	Theoretical Ratio
5	2.9	4.17
9	0.8[a]	2.38
12	1.4	1.78
15	1.2	1.33

[a]Subject to large errors, as discussed in Ref. 51.

V. FISSION-PRODUCT STUDIES

A. ENDF/B-IV GAMMA AND BETA SPECTRA (T. R. England and N. L. Whittemore)

A code was prepared to abstract beta end-point energies, gamma energies, internal conversion coefficients, and all associated intensities from ENDF/B-IV decay files. These data were used to calculate Q values and the average beta, total gamma, internal conversion, and average neutrino energies for the 180 nuclides having spectral data in ENDF/B-IV (711 nuclides in the files are unstable; the 180 nuclides having spectral data are those most important to decay heating). Each energy and Q-value was compared to values in ENDF/B-IV as one of several checks for file errors. Only 10 nuclides were found which differed from the file values by >1% for average beta and total gamma energies, but 63 of the calculated Q-values were outside the uncertainty range of the experimental Q-values. Table IV lists those nuclides found to be in significant error along with the corrections made in the LASL files. Table V lists the percent differences in average beta, total gamma, and Q-value for 69 nuclides; only these were found to differ from the file values by $\geq$ 1%.

TABLE IV

NUCLIDES HAVING TYPOGRAPHICAL OR SUSPECTED ERRORS IN ENDF/B-IV FISSION PRODUCT FILES

Nuclide	Comments
^{97}Y	$\bar{E}_\gamma = 9.35 \times 10^5$ eV.
^{104m}Rh	Normalization factor (F) = 0 (F should be 1.8535×10^{-2}), and typographical errors in spectra.
^{126}Sn	$\tau_{1/2} = 3.15569 \times 10^{12}$ s.
^{129m}Te	Internal conversion energy of 0.6682×10^5 eV added to $\bar{E}_\gamma$.
^{130m}Sb	$\bar{E}_\gamma$ too small ($E_\gamma \cong 3.04 \times 10^6$ eV). Change normalization to 1.17717.
^{131}Sb	$\bar{E}_\gamma = 1.7025 \times 10^6$ eV.
^{133}Sb	$\bar{E}_\gamma$ too large ($E_\gamma \cong 2.5 \times 10^6$ eV). Change normalization to 3.87351×10^{-1}.
^{136}Cs	$\bar{E}_\gamma$ includes some γ energy from ^{136}Ba.
^{138m}Cs	$\bar{E}_\gamma$ too small ($\bar{E}_\gamma \cong 2.6 \times 10^6$ eV). Change normalization to 1.23827.
^{140}La	$\bar{E}_\gamma$ too small ($\bar{E}_\gamma \cong 2.3 \times 10^6$ eV). Change normalization to 1.03275.
^{142}La	$\bar{E}_\gamma$ too large ($E_\gamma \cong 2.4 \times 10^6$ eV). Change normalization to 0.96470.
^{152m}Pm	$\bar{E}_\beta$ too small ($\bar{E}_\beta \cong 0.9 \times 10^6$ eV) and beta intensities do not sum to 1.0. Change normalization to 2.14551.
^{166}Er	σ(0.0253 eV) too large ($\sigma \cong 20$ b).

ENDF/B-IV contains internal conversion ratios for only 38 nuclides. The fractional transition energy of internal conversion was calculated and compared with fractions from Ref. 53; the following nine nuclides differed significantly: ^{90m}Zr, ^{99}Mo, ^{111}Pd, ^{125m}Te, ^{132}Te, ^{133m}Te, ^{133}Xe, ^{137m}Ba, and ^{144}Ce. The code used in these data tests will be extended to generate group spectral data for CINDER.

TABLE V

PERCENT DIFFERENCE OF CALCULATED AND ENDF B-IV ENERGIES

Nuclide	Beta	Gamma	Q	MAT
32-Ge- 79	2.7448E-04	1.9892E-03	4.7759E+00	58
33-As- 80	4.0677E-05	-3.7192E-03	2.2196E+00	73
33-As- 82M	7.2115E-05	2.2451E-04	-1.4771E+00	76
34-Se- 83	-2.9167E-04	5.9450E-04	4.6531E+00	95
36-Kr- 85	-1.0136E+01	3.0188E-02	-1.2631E-05	138
36-Kr- 90	3.0660E-04	7.9469E-04	3.6924E+00	144
36-Kr- 91	-6.8009E-06	6.8135E-04	3.9607E+00	145
36-Kr- 92	1.2599E-04	6.1166E-04	1.2635E+00	146
37-Rb- 89	4.2654E-04	8.2531E-04	1.2009E+00	158
37-Rb- 90	-1.4766E-04	5.7360E-04	1.4906E+00	159
37-Rb- 90M	3.7578E-05	7.6329E-05	1.9734E+00	160
37-Rb- 91	-7.7900E-05	3.2563E-04	2.4179E+00	161
38-Sr- 89	-2.6695E+00	0.	0.	176
37-Rb- 92	-4.1619E-05	9.0829E-04	1.2436E+00	162
38-Sr- 90	-1.2880E+01	0.	0.	177
39- Y- 90M	-1.0602E+01	7.4495E-04	9.9419E-03	195
39- Y- 91	-2.6235E+00	-9.0226E-02	-6.2550E-02	196
39- Y- 97	2.8741E-04	0.	2.2500E+00	204
40-Zr- 97	2.7685E-05	1.7076E-04	-2.9961E+00	223
41-Nb-100	2.7847E-05	4.8797E-04	3.4366E+00	249
42-Mo- 99	-4.0978E-04	-1.6590E-03	1.4811E+00	269
42-Mo-101	-4.3919E-04	2.2581E-03	3.4777E+00	271
43-Tc-102	-1.7668E-04	-9.9914E-02	-5.2810E+00	290
43-Tc-102M	-2.9572E-05	2.9894E-04	-1.8667E+00	291
44-Ru-105	1.0703E-03	1.1740E-03	2.4885E+00	314
44-Ru-106	3.8099E-03	0.	-1.0152E+00	315
45-Rh-104M	GAMMA NORMALIZATION = 0			333
45-Rh-107	4.1832E-04	1.6172E-02	-2.5466E+00	338
45-Rh-108	3.4277E-04	3.9059E-03	7.3451E+00	339
46-Pd-109	8.2231E-04	1.0792E+00	-1.7634E-03	364
46-Pd-111M	2.1737E-04	1.1616E-03	-1.1504E+00	368
49-In-120	3.9735E-04	6.5366E-05	4.8483E+00	461
50-Sn-125M	5.9857E-04	8.5709E-04	-2.4605E+00	497
50-Sn-126	4.5987E-05	4.8951E-04	-4.3679E+00	501
51-Sb-125	-2.6452E+00	3.5411E-05	4.6129E-01	518
51-Sb-126	2.8998E-04	2.8423E-04	-1.7217E+00	522
51-Sb-129	1.1731E-03	7.7591E-04	-2.7130E+00	524
51-Sb-130M	-1.1613E-04	2.8220E-04	-1.3559E+01	526
51-Sb-131	-6.8157E-05	1.6601E-04	3.3769E+00	527
51-Sb-132	1.0107E-04	-2.9851E-02	-2.7614E+00	528
51-Sb-132M	1.9474E-04	8.3391E-04	-3.1042E+00	529
51-Sb-133	-3.1393E-05	-9.1311E-04	1.5971E+01	530
52-Te-129M	-2.1712E-03	5.4827E-01	-1.0196E+01	549
52-Te-131	1.7740E-05	1.1748E-02	-4.8915E+00	551
52-Te-132	-1.1752E-03	1.7694E-03	-4.2367E+00	553
52-Te-133	6.8036E-04	3.8290E-04	1.8239E+00	554
52-Te-134	2.1995E-03	-1.9244E-04	-6.1786E+00	556
53- I-132	6.4542E-05	3.0953E-04	1.1408E+00	571
53- I-133	7.0722E-04	7.8874E-03	1.0093E+00	572
53- I-134	-2.5812E-05	1.8022E-03	4.7493E+00	574
53- I-135	1.2609E-03	3.0077E-03	-3.6846E+00	576
54-Xe-131M	0.	-2.1129E-03	2.2000E+00	593
54-Xe-139	4.8673E-04	3.4517E-03	1.6416E+00	604
55-Cs-136	3.8841E-03	3.4464E-04	1.3737E+01	618
55-Cs-138M	1.1397E-04	6.6677E-05	-9.9627E+00	621
55-Cs-140	4.2475E-05	2.4339E-03	2.4425E+00	623
56-Ba-141	7.7233E-04	2.1252E-03	3.3463E+00	644
57-La-140	1.0555E-03	4.1911E-04	-5.1363E+00	658
57-La-142	4.0828E-04	9.3736E-04	7.3065E+00	660
58-Ce-145	2.4325E-04	4.2966E-03	-4.5409E+00	679
58-Ce-146	-1.5781E-03	1.2829E-03	-3.3052E+00	680
59-Pr-144M	-1.5544E+00	-7.3665E-03	-1.9835E-03	697
59-Pr-146	4.6263E-04	2.2564E-03	-4.7779E+00	699
60-Nd-147	-1.3405E-03	-3.6071E-03	-5.9412E+00	718
60-Nd-149	1.0383E-03	1.7705E-03	-4.0023E+00	720
61-Pm-147	4.7086E-03	-2.6400E+00	8.9087E-02	733
61-Pm-148	-2.1991E-04	8.0112E-04	1.0602E+00	734
61-Pm-151	-9.6493E-04	1.8540E-04	1.6248E+00	738
61-Pm-152M	-3.9179E-04	-2.8464E-05	-3.4860E+01	740

B. Summary of Major Nuclide Data in ENDF/B-IV (T. R. England, R. E. Schenter [Hanford Engineering Development Lab], and N. L. Whittemore

The ENDF/B-IV fission product and decay data files contain >300 000 card images (~4000 pages are required for a computer listing). Partly for use as a compact source of reference data and partly for use in ENDF documentation, Ref. 54 was completed during this quarter. It contains the major parameters of interest to many users in a 27-page table in a readable format. In particular, each of the 824 nuclides classed as fission products have the following parameters listed: σ_{th}, RI, $\tau_{1/2}$, $\overline{E}_\beta$, $\overline{E}_\gamma$, $\overline{E}_\alpha$, decay and (n,γ) branching fractions, Q, AWR, type of decay (RTYP), final state (RFS), number of decay modes (NDK) and number of spectra (NSP). The few known file errors have been corrected.

C. Processing of Fission-Product Capture Cross Sections (W. B. Wilson, T. R. England, M. G. Stamatelatos, and R. J. LaBauve)

Of the 824 fission products of the ENDF/B fission-product tape, 181 are complete with cross-section data in MF = 3. The capture reaction cross sections of these 181 isotopes are being processed in 4 energy groups via several intermediate steps.

The ENDF/B cross sections are first processed by MINX to produce PENDF files of Doppler-broadened pointwise cross sections at 10^3°K. PENDF files are stored on Photostore.

Using PENDF files as input, multigroup cross sections are to be processed in approximately 150 groups by MINX, using a flux spectrum for an equilibrium-loaded Pressurized Water Reactor (PWR) at midlife.[55] The choice of this group structure is presently underway.

The 4-group cross sections are obtained by collapsing the 150-group values with the PWR flux spectrum. A collapsing routine COLAPS has been written and is presently being debugged. The routine accepts flux weighting function input as histogram data or log-log interpolation points; a functional form[56] is also available in a built-in module.

D. CSEWG Fission-Product Yield Meeting (T. R. England)

A meeting on fission-product yields was hosted by LASL on September 23, 1975. The intent of the meeting was to discuss the fissionable nuclide yield sets, yield charge distribution model, and new source data to be included in Version V of ENDF/B. The meeting was well attended; six people from LASL and eleven from other Laboratories participated.

A preliminary set of yields for Version-V was discussed and numerous tables were presented. As noted in earlier progress reports, the delayed neutron calculations are particularly sensitive to changes in the yield distribution. The preliminary Version-V results are compared with ENDF/B-IV calculations and evaluations in Table VI. Table VII compares the yield-weighted charge deviation from the fissionable nuclide charge and also the total energy release for fission. The latter comparison is essentially a consistency check. Evaluated yields are not adjusted to conserve energy; a 0.09% change in the yield-weighted stable mass ($\overline{MS}$) or a 0.21 amu mass unit error in $\overline{\nu}_p$ is sufficient to account for the nominal 200 MeV/fission. The same quantity when calculated with the evaluated $\overline{\nu}_d$ and $\overline{\nu}_p$ values (tabulated in Table VI) results in energy release values between -588 and +781 MeV/fission for the differing fissionable nuclides. The energies using only calculated $\overline{\nu}_d$, $\overline{\nu}_p$, and $\overline{MS}$ values are, therefore, surprisingly consistent.

There are ten yield sets in ENDF/B-IV. There was a tentative agreement that as many as 23 sets should be incorporated into Version-V. Ben Rider from General Electric (GE) has agreed to attempt a preliminary evaluation of several additional sets using his evaluation code; this will require input from LASL on the parameters to be used in the charge distribution model.

Two committees were formed, one to study the direct yield distribution and one to specify yield uncertainties.

More detailed results of the yield meeting were reported at the Fall CSEWG Meeting at BNL in October.

E. Actinide Chains (M. Bjerke [Oregon State University], T. R. England, and N. L. Whittemore)

A preliminary set of actinide chains was prepared for use in the CINDER code. The chains are extensive, but improved cross-section data are needed for several actinides before release for general usage.

F. Damage Assessment from a Nuclear Reactor Accident (J. C. Rodgers [H-DO], T. R. England, and N. L. Whittemore)

LASL's H-Division is engaged in a method to assess the damages due to a spread of radioactive con-

TABLE VI

DELAYED AND PROMPT NEUTRON COMPARISONS[a]

9-75

	$\bar{\nu}_d$/100 FISSIONS			$\bar{\nu}_p$		
	CALCULATION			CALCULATION		
FISSION NUCLIDE	ENDF/B-IV	ENDF/B-VA	ENDF/B-IV EVALUATION	ENDF/B-IV	ENDF/B-VA	ENDF/B-IV EVALUATION
$^{235}U(T)$	1.604	1.547	1.67 ± 0.07	2.41	2.38	2.40
$^{235}U(F)$	1.483	1.735	1.67 ± 0.07	2.38	2.42	2.53–2.65
$^{235}U(HE)$	1.095	1.034	0.90 ± 0.1	3.63	4.17	4.38–4.51
$^{238}U(F)$	2.934	3.013	4.60 ± 0.25	2.70	3.06	2.43–2.58
$^{238}U(HE)$	1.963	1.972	2.60 ± 0.2	4.02	4.44	4.43–4.58
$^{239}Pu(T)$	0.520	0.610	0.645 ± 0.04	2.92	2.92	2.87
$^{239}Pu(F)$	0.508	0.589	0.645 ± 0.04	2.77	2.82	3.01–3.15
$^{241}Pu(T)$	1.047	1.232	1.57 ± 0.15	3.00	2.99	2.92
$^{233}U(T)$	0.821	0.777	0.740± 0.04	2.47	2.45	2.49
$^{232}Th(F)$	3.933	4.833	5.27 ± 0.4	2.39	2.45	1.99–2.11

[a] Calculated values use ENDF/B yields and branching fractions.

Uncertainties on $\bar{\nu}_d$ are taken from a review by S. A. Cox (ANL/NDM-5, April 1974). The evaluated $\bar{\nu}_p$ values apply at 0.0253 eV for thermal (T) fission; 1.0 and 2.0 MeV for fast (F) fission, and 14 and 15 MeV for high energy (HE) fission.

tamination from a reactor accident. This involves the inventory of isotopes from several representative types of reactors, along with the need to estimate the fractional release rates from various accidents, meteorological modeling, etc. T-2 has provided assistance in the inventory estimates by supplying data and helping to form the nuclide chains in a format acceptable to the CINDER-7 code.[57] Preliminary calculations by J. C. Rodgers using the code and chain data indicated that the Liquid Metal Fast Breeder Reactor (LMFBR) inventories of ^{90}Sr, ^{137}Cs, and ^{85}Kr published in WASH-1535 are in error by factors of 4, 4.5, and 2, respectively. Such large differences cannot be explained on the basis of the new data supplied for the calculations. Simple desk calculations indicate that the WASH-1535 results (Table 4.2-12 of the report) are in error. Inventory comparisons with WASH-1400 for Light Water Reactors are in reasonably good agreement.

G. Fission Yield Theory (C. W. Maynard [University of Wisconsin], T. R. England, and P. G. Young)

Significant progress has been made in the last few years in understanding the fission process. This has resulted in a general understanding of the dominance of asymmetric fission. However, the theory implemented to date has not resulted in good values for the yields of the various fragments resulting from different modes of fission. The theoretical concepts available have not been fully implemented and there is a good possibility that very acceptable results can be obtained by a careful calculational program. In particular, use of a statistical theory of fission employing a single-particle corrected semiempirical atomic mass formula and a numerically evaluated convolution of level densities based on a partition function model is indicated as a likely calculation model.

TABLE VII

COMPARISON OF CHARGE DEVIATION AND ENERGY RELEASE BASED ON ENDF/B-IV AND -VA YIELD WEIGHTINGS

9-75

FISSION NUCLIDE	$\leftarrow \lvert Z_f - \bar{Z} \rvert \rightarrow$ ENDF/B-IV	ENDF/B-VA	TOTAL ENERGY RELEASE/FISSION[a] (MeV) ENDF/B-IV	ENDF/B-VA
$^{235}U(T)$	0.008	0.016	181	206
$^{235}U(F)$	0.015	0.004	177	186
$^{235}U(HE)$	0.073	0.008	115	190
$^{238}U(F)$	0.030	0.012	152	166
$^{238}U(HE)$	0.070	0.033	115	146
$^{239}Pu(T)$	0.015	0.016	190	189
$^{239}Pu(F)$	0.005	0.029	200	176
$^{241}Pu(T)$	0.005	0.009	193	208
$^{233}U(T)$	0.003	0.023	189	171
$^{232}Th(F)$	0.013	0.249	143	358

[a] $E = 931.481x[M_f + M_n(1-\bar{\nu}_p-\bar{\nu}_d)-\overline{MS}]$

Note that 200 MeV = 0.2147 amu

A survey of the literature indicated the simple statistical model of fission as developed by Fong[58] gives a qualitatively useful mode, but that it is inadequate in its present form. However, the necessary components for carrying out a more sophisticated treatment of the model as outlined in the preceding paragraph is available. The "Semiempirical Atomic Mass Formula" developed by Seeger and Howard[59] is available in a useful format on magnetic tape and can be used in conjunction with a level density program. Ford[60] has a level density program which can be modified to carry out the fission yield calculation. These modifications are currently being studied.

VI. MEDIUM ENERGY LIBRARY (D. G. Foster, Jr.)

Several additions have been made to NASPRO, the processor for converting Monte Carlo interaction histories to the NASA/Langley working format of equiprobability boundaries. We are attempting to transmit the output directly in binary form on 7-track magnetic tape. The format of the tape library has been worked out and approved by NASA, and a library manager added to NASPRO to add the data from each run to the library. For the initial library, only data calculated using incident protons will be used. Accordingly, NASPRO has been modified to generate incident-neutron data from incident-proton results by applying the isosinglet approximation to the output from the cascade phase of the histories. Both sets are then added to the library.

The library normally resides on the HYDRA disk with card backup. In order to reduce the bulk of the printout from NASPRO and facilitate sending copies to NASA, the output has been divided into an Express file and a Detail file. Both files are stored on Photostore and dumped to microfiche. If these steps are successful, only the Express file is actually printed. The binary library is also dumped to Photostore periodically to reduce dependence on card backup.

The original intention was to send NASA a working library immediately, to be followed later by an archival library in which the data would be reduced to differential cross sections. The final library was also to contain miscellaneous additional data on heavy charged particles, the excitation and recoil energies of the residual nucleus, and the distribution of spallation products. The present plan is for us to develop a simple program for calculating differential cross sections by fitting quadratic surfaces to the equiprobability bins from the working library. Since this will eliminate any need for a separate archival library, the working library will contain all of the supplementary information.

Production runs have been completed for ^{16}O bombarded by 20-3500 MeV protons. Since the decision to abandon the archival library was made after production runs began, data on spallation products were subsequently keypunched from the printouts and added to the library in a separate operation. Future production runs will supply this material directly to the library. The oxygen library will be shipped to Langley shortly for tests of the transmission procedure and format.

REFERENCES

1. B. Zeitnitz, H. Dubenkropp, R. Putzki, G. J. Kirouac, S. Cierjacks, I. Nebe, and Carl B. Dover, "Neutron Scattering from ^{15}N," Nucl. Phys. A166, 443 (1971).

2. C. F. Sikkema, "Energy Levels in ^{16}N from $^{15}N(n,n)^{15}N$ Elastic Scattering," Nucl. Phys. 32, 470 (1962).

3. G. M. Hale, "R-Matrix Analysis of the Light Element Standards," Invited paper, Conf. on Nucl. Cross Sections and Tech., Washington, D. C. (March 1975).

4. H.-H. Knitter, private communication, 1975.

5. P. A. Moldauer, "Statistical Theory of Nuclear Cross Sections," Phys. Rev. B642, 135 (1964).

6. L. Milazzo-Colli and G. M. Braga-Marcazzan, "α-Emission by Pre-equilibrium Processes in (n,α) Reaction," Nucl. Phys. A210, 297 (1973).

7. G. M. Braga-Marcazzan, E. Gadioli-Erba, L. Milazzo-Colli, and P. G. Sona, "Analysis of the Total (n,p) Cross Sections Around 14 MeV with the Pre-equilibrium Excitation Model," Phys. Rev. C6, 1398 (1972).

8. C. M. Perey and F. G. Perey, "Compilation of Phenomenological Optical Model Parameters, 1969-1972," Atomic Data and Nuclear Data Tables 13, 293 (1974).

9. C. S. Mani, M. A. Melkanoff, I. Iori, "Neutron Penetrabilities Using an Optical Model Potential," Commissariat A L'Energie Atomique report CEA 2380 (1963).

10. J. Frehaut and G. Mosinski, "Measurement of (n,2n) and (n,3n) Cross Sections for Incident Energies between 6 and 15 MeV," Conf. on Nucl. Cross Sections and Tech., Washington, D. C. (March 1975).

11. B. P. Bayhurst, J. S. Gilmore, R. J. Prestwood, J. B. Wilhelmy, N. Jarmie, B. H. Erkkila, and R. A. Hardekopf, "Cross Sections for (n,xn) Reactions between 7.5 and 28 MeV," Phys. Rev. C12, 451 (1975).

12. W. Dilg, H. Vonach, G. Winkler, and P. Hille, "Messung Von(n,2n) Wirkungsquerschnitten an Schweren Kernen," Nucl. Phys. A118, 9 (1968).

13. D. R. Nethaway, "Cross Sections for Several (n,2n) Reactions at 14 MeV," Nucl. Phys. A190, 635 (1972).

14. S. M. Qaim, "Total (n,2n) Cross Sections and Isomeric Cross Section Ratios at 14.7 MeV in the Region of Rare Earths," Nucl. Phys. A224, 319 (1974).

15. L. R. Veeser, Los Alamos Scientific Laboratory, private communication, 1975.

16. B. M. Carmichael, "Standard Interface Files and Procedures for Reactor Physics Codes, Version III," Los Alamos Scientific Laboratory report LA-5486-MS (1974).

17. O. Ozer, Ed., "Description of the ENDF/B Processing Codes and Retrieval Subroutines," Brookhaven National Laboratory report BNL-50300 (ENDF 11) (June 1971).

18. P. Rose, Brookhaven National Laboratory, private communication, 1975.

19. D. E. Cullen, "Program SIGMA1 (Version 74-1)," Lawrence Livermore Laboratory report UCID-16426 (January 1974).

20. K. D. Lathrop, "DTF-IV, A FORTRAN-IV Program for Solving the Multigroup Transport Equation with Anisotropic Scattering," Los Alamos Scientific Laboratory report LA-3373 (1965).

21. R. Schenter, Hanford Engineering Development Lab, private communication, 1975.

22. E. D. Cashwell, J. R. Neergaard, W. M. Taylor, and G. D. Turner, "MCN: A Neutron Monte Carlo Code," Los Alamos Scientific Laboratory report LA-4571 (1972).

23. R. J. LaBauve, C. R. Weisbin, R. E. Seamon, M. E. Battat, D. R. Harris, P. G. Young, and M. M. Klein, "PENDF: A Library of Nuclear Data for Monte Carlo Calculations Derived from Data in ENDF/B Format," Los Alamos Scientific Laboratory report LA-5687 (1974).

24. K. D. Lathrop, "GAMLEG -- A FORTRAN Code to Produce Multigroup Cross Sections for Photon Transport Calculations," Los Alamos Scientific Laboratory report LA-3267 (1965).

25. J. H. Hubbell, W. J. Veigele, E. A. Briggs, R. T. Brown, D. T. Cromer, and R. J. Howerton, "Atomic Form Factors, Incoherent Scattering Functions, and Photon Scattering Cross Sections," to be published in J. Phys. Chem. Ref. Data 4, (1975).

26. D. J. Dudziak, R. E. Seamon, and D. V. Susco, "LAPHANO: A P_0 Multigroup Photon-Production Matrix and Source Code for ENDF," Los Alamos Scientific Laboratory report LA-4750-MS (ENDF-156) (1967).

27. D. J. Dudziak, A. H. Marshall, and R. E. Seamon, "LAPH: A Multigroup Photon Production Matrix and Source Vector Code for ENDF/B," Los Alamos Scientific Laboratory report LA-4337 (1970).

28. D. J. Dudziak, "ENDF Formats and Procedures for Photon Production and Interaction Data (ENDF-102, Vol. II)," Los Alamos Scientific Laboratory report LA-4549 (1971).

29. M. G. Stamatelatos, R. J. LaBauve, and J. C. Vigil, Nuclear Data Processing for HTGR Safety Research, in "Quarterly Report on Transport Theory, Reactor Theory, and Reactor Safety for the Period April 1 - June 30, 1975," K. D. Lathrop, Person-in-Charge, Los Alamos Scientific Laboratory report LA-6029-PR, pp. 18-21 (August 1975).

30. B. J. Toppel, A. L. Rago, and D. M. O'Shea, "MC^2, A Code to Calculate Multigroup Cross Sections," Argonne National Laboratory report ANL-7318 (1967).

31. W. W. Clendenin, "Calculation of Thermal Neutron Diffusion Length and Group Cross Sections: The GLEN Program," Los Alamos Scientific Laboratory report LA-3893 (1968).

32. W. W. Clendenin, "Calculation of Thermal Neutron Scattering Cross Sections for Crystalline Materials: The TOR Program," Los Alamos Scientific Laboratory report LA-3823 (1967).

33. Y. D. Naliboff and J. U. Koppel, "HEXSCAT, Coherent Elastic Scattering of Neutrons by Hexagonal Lattices," General Atomic report GA-6026 (1964).

34. D. R. Harris, R. J. LaBauve, R. E. MacFarlane, P. D. Soran, C. R. Weisbin, and J. E. White, "MINX, A Modular Code System for Processing Multigroup Cross Sections from Nuclear Data in ENDF/B-Format," Proc. of Seminar on Codes for Nuclear Data Processing, NEA-CPL Ispra (1973).

35. R. W. Hardie and W. W. Little, Jr., "1DX, A One-Dimensional Diffusion Code for Generating Effective Nuclear Cross Sections," Battelle Northwest Laboratory report BNWL-954 (1969).

36. R. J. LaBauve, Los Alamos Scientific Laboratory, unpublished data, 1975.

37. P. Wälti, "Evaluation of Grain Shielding Factors for Coated Fuel Particles," Nucl. Sci. Engr. 45, 321-330 (1971).

38. P. Wälti and P. Koch, "MICROX, A Two-Region Flux Spectrum Code for the Efficient Calculation of Group Cross Sections," Gulf General Atomic report GA-A10827 (1972).

39. C. A. Stevens and C. V. Smith, "GAROL, A Computer Program for Evaluating Resonance Absorption Including Resonance Overlap," General Atomic report GA-6637 (1965).

40. D. R. Mathews, P. K. Koch, J. Adir, and P. Wälti, "GGC-5, A Computer Program for Calculating Neutron Spectra and Group Constants," Gulf General Atomic report GA-8871 (1971).

41. K. M. Case, F. De Hoffman, and G. Plazek, Introduction to the Theory of Neutron Diffusion, U. S. Government Printing Office, Washington, D. C. (1953).

42. I. Carlvik, "Dancoff Correction in Square and Hexagonal Lattices," Aktiebolaget Atomenergi report AE-257 (1966).

43. I. Carlvik and B. Pershagen, "The Dancoff Correction in Various Geometries," Aktiebologet Atomenergi report AE-16 (1959).

44. E. P. Wigner, E. Creutz, J. Jupnik, and T. Snyder, "Resonance Absorption of Neutrons by Spheres," J. Appl. Phys. 26, 260 (1955).

45. M. M. Levine, "Resonance Integral Calculations for ^{238}U Lattices," Nucl. Sci. and Eng. 16, 271 (1963).

46. J. M. Otter, "Escape Probability Approximations in Lumped Resonance Absorbers," Atomics International report NAA-SR-9744 (1964).

47. G. I. Bell and S. Glasstone, Nuclear Reactor Theory (Van Nostrand Reinhold Company, New York, 1970)

48. L. Dresner, Resonance Absorption in Nuclear Reactors (Pergamon Press, New York, 1960).

49. P. G. Young and D. G. Foster, Jr., " A Preliminary Evaluation of the Neutron and Photon-Production Cross Sections for Oxygen," Los Alamos Scientific Laboratory report LA-4780 (1972).

50. P. G. Young and D. G. Foster, Jr., "A Preliminary Evaluation of the Neutron and Photon-Production Cross Sections for Aluminum," Los Alamos Scientific Laboratory report LA-4726 (1972).

51. D. W. Muir and J. M. Bunch, "High Energy Proton Simulation of 14-MeV Neutron Damage in Al_2O_3," to be published in the Proc. of the Gatlinburg Conf. on Radiation Damage in Fusion Reactor Materials, October 1-5, 1975.

52. D. M. Parkin and A. N. Goland, "A Computational Method for the Evaluation of Radiation Effects Produced by CTR-Related Neutron Spectra," Brookhaven National Laboratory report BNL-50434 (1974).

53. A. Tobias, "Data for the Calculation of Gamma Radiation Spectra and Beta Heating from Fission Products (Revision 3)," Central Electricity Generating Board Research Department, Berkeley Nuclear Laboratories report RD/B/M2669 CNDC(73) P4 (June 1973).

54. T. R. England and R. E. Schenter, "ENDF/B-IV Fission Product Files: Summary of Major Nuclide Data," Los Alamos Scientific Laboratory report LA-6116-MS (October 1975).

55. N. G. Demas, Westinghouse Electric Corporation, Nuclear Energy Systems, private communication. 1975.

56. R. W. Roussin, Oak Ridge National Laboratory, private communication, 1975.

57. T. R. England, R. Wilczynski, and N. L. Whittemore, "CINDER-7: An Interim Report for Users," Los Alamos Scientific Laboratory report LA-5885-MS (April 1975).

58. P. Fong, Statistical Theory of Nuclear Fission (Gordon and Breach, Science Publishers, Inc., New York, 1969).

59. P. A. Seeger and W. M. Howard, "Semiempirical Atomic Mass Formula," Nucl. Phys. A238, 491-532 (1975).

60. G. P. Ford, "Calculation of Nuclear Level Densities for ^{56}Fe, ^{59}Co, ^{60}Ni, ^{61}Cu, ^{62}Ni, ^{63}Cu, and ^{65}Cu," submitted for publication in Phys. Rev. C (1975).